

CHAPTER II

THEORETICAL BACKGROUND

The theory related to the fundamental properties of the barium titanate, Fe-doped barium titanate, calcium copper titanate and Fe-doped calcium copper titanate films will be presented. The sol-gel processing used to prepare these films in this research is presented in this chapter. The gamma ray and interactions between gamma ray and the materials will be also presented in this chapter. The last of this, the formula for thickness determination from transmission data will be derived.

2.1 Barium titanate, Fe-doped barium titanate, calcium copper titanate and calcium copper titanate thin films

2.1.1 Barium titanate (BTO)

Barium titanate (BaTiO_3), which was discovered 60 years ago, is a ferroelectric material that has gained much interest due to its many potential applications, such as high dielectric constant capacitors, dynamic random access memories, and piezoelectric and optical wave guide devices [17, 18, 19]. BTO is a perovskite material which is a typical ABO_3 where as Ba ion (Ba^{2+}) is at the A-sites and Ti ion (Ti^{4+} as B) is at the B-sites. In Fig. 2.1, barium atoms are occupied at the eight corners of the cube, oxygen atoms are occupied at the faces, titanium atom

is at the center of the cube. A crystal structure of barium titanate depends on the temperature range [20]. At room temperature a tetragonal BTO is the most stable phase [21, 22]. A Curie temperature (T_c) of BTO, which is a temperature at which a tetragonal phase transform into a cubic phase, is about 120 °C [23]. The lattice parameters of bulk BTO are 3.994 Å and 4.038 Å for the a-axis and c-axis [24].

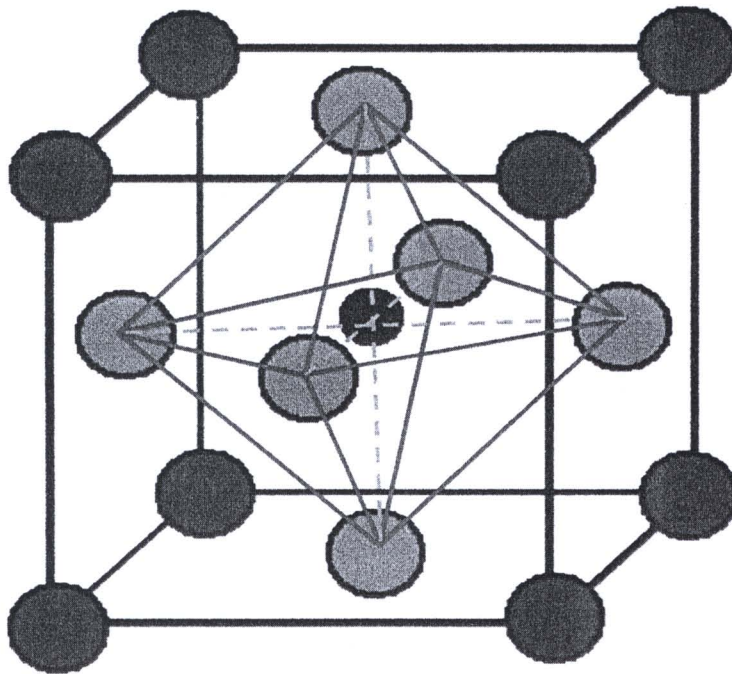


Figure 2.1: Unit cell structure of the BTO, with Ba atom in dark red, Ti atom in black and O atom in blue.

2.1.2 Fe-doped barium titanate (Fe-doped BTO)

Many research groups have been interested in optical properties of Fe-doped BTO. In 2002, Maier et al. studied structural and physical properties of ferroelectric and ferrimagnetic on $\text{BaFe}_x\text{Ti}_{1-x}\text{O}_3$ (BFTO) thin film with $0.5 \leq x \leq 0.75$ and compared with those of BTO films under identical conditions [25]. They found that the replacement of 50% or more of Ti by Fe deteriorates the crystalline quality, leading to ferrimagnetic ordering well above room temperature, and BTO could be converted from an n-type to a p-type semiconductor. Stashans et al. investigated simulation of iron impurity in BTO crystals. They found that the equilibrium spatial configurations obtained for both cubic and tetragonal structures change in atomic interaction between the impurity atom and its surrounding O atoms. It is observed that the Fe atom has practically only covalent bonding with the four O atoms situated around it within the xy plane, while the interaction with the two oxygens along the z-axis is purely ionic [26].

2.1.3 Calcium copper titanate (CCTO)

Calcium copper titanate ($\text{CaCu}_3\text{Ti}_4\text{O}_{12}$) is a perovskite-like body centered cubic structure with a lattice parameter $a = 7.391 \text{ \AA}$ [27]. Home et al. found that there were no any structural phase transition of CCTO from 100 K to 600 K [28]. Figure 2.2 shows the unit cell of CCTO, where Ca and Cu ions are occupied at A-sites and Ti cations reside at the B-site. CCTO has been studied in many research group due to its high dielectric constant about 10^4 for polycrystal [29, 30, 31] and 10^5 for single crystal [29] at room temperature. The high dielectric constant properties of CCTO are important in designing novel microelectronics such as microelectronic devices [30, 32, 33], memory devices [31], dynamic random access memories [31].

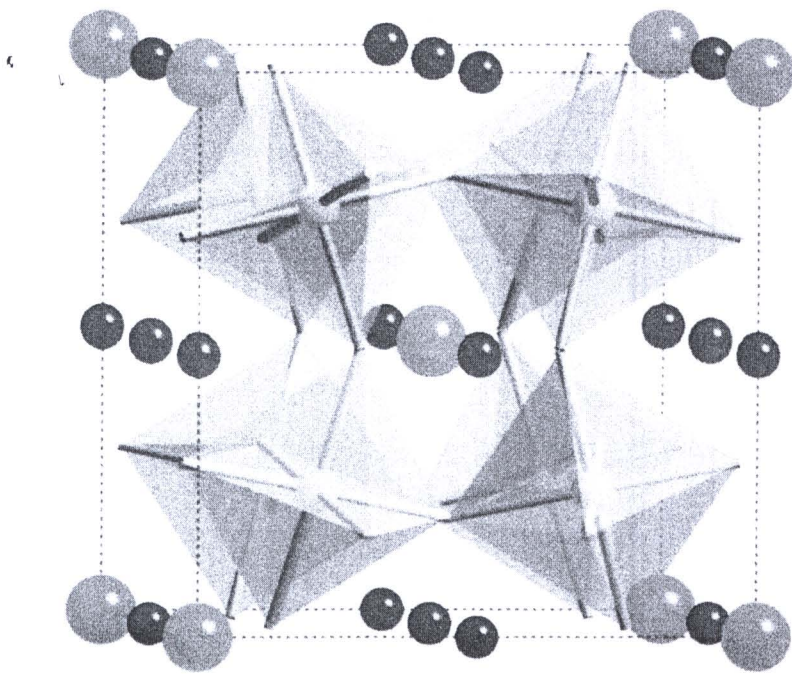


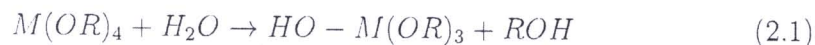
Figure 2.2: Unit cell structure of CCTO, with Ca atom in green, Cu atom in blue and TiO₆ octahedral in teal [27].

2.1.4 Fe-doped calcium copper titanate (Fe-doped CCTO)

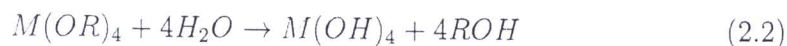
In 2009, Krohns et al. showed correlations of structural, magnetic, and dielectric properties of undoped and doped CCTO [34]. They reported that dielectric constant of CCTO versus temperature increase after $\text{CaCu}_3\text{Ti}_{4-x}\text{Fe}_x\text{O}_{12}$ in the frequency range from 1 kHz to 1 MHz. The intrinsic relaxation showing up at higher temperatures in Fe-doped CCTO seems to correspond to the single intrinsic relaxation observed in the Mn-doped sample.

2.2 Sol-Gel processing

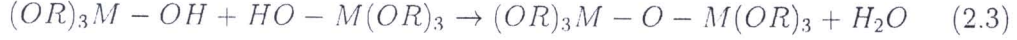
The definition of *sol* and *gel* will be mentioned before we described about sol-gel process. A *sol* is a colloidal suspension of solid particles in a liquid and *gel* is a substance that contains a continuous solid skeleton enclosing a continuous liquid phase. *Gel* can also be formed from particulate sols [35], when attractive dispersion forces cause them to stick together in such a way as to form a network polymers. A precursor (starting material) of the sol-gel process for preparation consist of a metal or metalloid element surrounded by various ligands (ligand is an ion or molecule that bond a central metal atom). Metal alkoxides are popular precursors because they react with water. The first step of a reaction is called hydrolysis as in the following reaction:



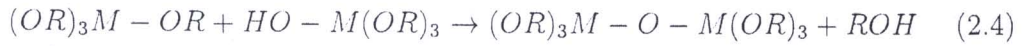
where R represents a ligand and ROH is an alcohol; M is metal; the bar (-) indicates a chemical bond. Depending on the amount of water and catalyst are present, hydrolysis may go to completion (so that all of the OR groups are replaced by OH)



and then two partially hydrolyzed molecules can link together in a condensation reaction;



or



By definition, condensation creates a small molecule (such as water or alcohol). This reaction can continue to build larger and larger metal containing molecules by the process of polymerization. Followed by drying process, the water or alcohol from the condensation process is removed and then a volume reduction takes place. In this process the drying temperature should be high enough to remove the free alcohol, water, catalyst and other compound. The common temperature used in preheat process is about 100 °C - 200 °C [36, 37]. Most gels are amorphous (much noncrystalline), even after drying, but they could turn to be crystalline with heating at higher temperatures [36, 37]. It is necessary to heat or sinter the gel to a high enough temperature to produce crystalline material. Sintering is a process of collapse of pores driven by surface energy. Material moves by viscous flow or diffusion to eliminate porosity and reduce the solid-vapor interfacial. In amorphous materials, transport of atoms occurs by viscous flow; in crystalline materials sintering involves diffusion. For crystalline gels there are the further complications of grain growth and phase transformation.

2.3 Gamma ray

Gamma ray is an electromagnetic (EM) radiation as shown in Fig. 2.3. EM radiation differs in frequency and energy.

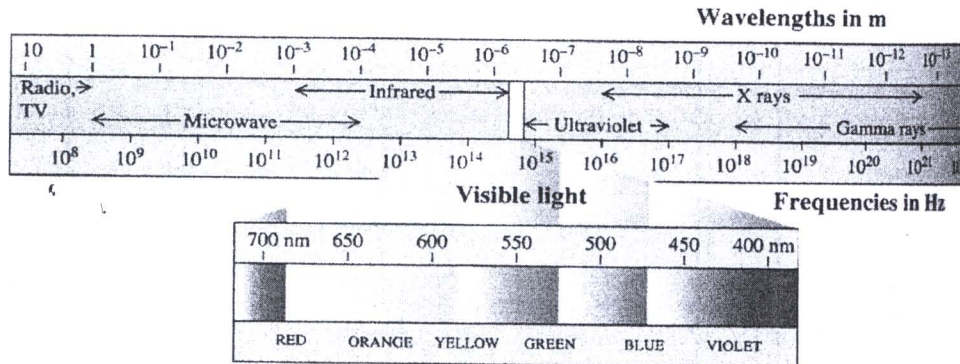


Figure 2.3: The electromagnetic spectrum.

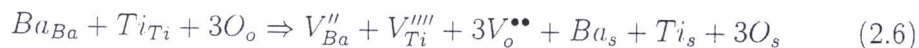
From Fig. 2.3, gamma rays have the wavelength less than 10^{-10} nm and the frequency more than 10^{18} Hz, respectively. They have the energy more than 10 keV and therefore they can penetrate more than other radiations such as alpha and beta rays [38]. Gamma ray was produced when a nucleus is placed in an excited state, either by bombardment with high energy particles or by a radioactive transformation, it can decay to the ground state. This process is called gamma decay shown in equation 2.5 for ^{60}Co .



where $^{60}\text{Co}^*$ is an excited state; ^{60}Co is a ground state and γ represent gamma ray.

2.4 Interactions between gamma ray and materials

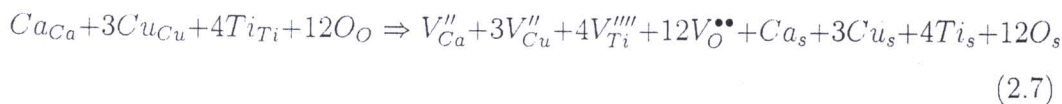
High energy electromagnetic radiation or high energy particles, such as X-rays, gamma rays, electron or neutron bombardment could change the physical properties of materials. Defects in material could be created when the high energy electromagnetic or particles have enough energy to overcome the Coulomb force between ions and break the chemical bond. A negative ion could be removed and this ion vacancy can subsequently trap an electron. This process is called oxygen vacancies (known as colour centers) or F centres (from Farbe, the German word for colour) presented in oxide material in form of Schottky or Frenkel defects. The colour centres are produced during high energy irradiation and they annihilated under the room temperature. Point equilibrium of colour centres for individual material depending on one particular dose rate and parameters of the material such as thickness [39] and dopant [39] can predict the behavior of those materials under different doses. There are two types of defects in barium titanate; the type that preserves the stoichiometry (Schottky) and the type that changes the stoichiometry that occurs at the dopant substituted cells. Oxygen vacancy defects are commonly found in BaTiO_3 due to an insufficient oxygen supply during the film processing [40]. Intrinsic Schottky defects in BTO are believed to form according to the following process: [15].



where Ba_{Ba} , Ti_{Ti} , 3O_{O} are occupied Ba, Ti and O sites, respectively, V''_{Ba} , V''''_{Ti} and $3V^{\bullet\bullet}_{\text{O}}$ are vacancies of Ba, Ti and O atoms, respectively, and Ba_{s} , Ti_{s} and 3O_{s} are the Schottky defects, respectively.



For CCTO under gamma irradiation;



where Ca_{Ca} , $3Cu_{Cu}$, $4Ti_{Ti}$, $12O_O$ are occupied Ca , Cu , Ti and O sites, respectively, V_{Ca}'' , $3V_{Cu}''$, $4V_{Ti}''''$ and $12V_O^{\bullet\bullet}$ are vacancies of Ca , Cu , Ti and O atoms, respectively, and Ca_s , $3Cu_s$, $4Ti_s$ and $12O_s$ are the Schottky defects, respectively.

Note that the notation from equation 2.6 and 2.7 is called Kröger-Vink notation, where A_A indicates that A-atom on an A-site; V_A denotes a vacancy on A-site; positive charge is marked by a point (e.g. V^{\bullet}), negative charge is marked by a hyphen or dash (e.g. V') to distinguish this relative charge from the absolute charge.

2.5 Thickness determination from transmission data

A method proposed in this thesis is to determine the thickness from the interference fringes of the transmission spectra. The concept of this method is based on the interference between the light reflecting from the film surface (1) and from the film-substrate interface (2) as shown in Fig. 2.4. The simplest ideal case to obtain perfect transmission spectra is that the film is perfectly flat and has a uniform thickness. The transmission (T) of the system depends on the parameters such as the optical constants, the film thickness, the wavelength of the light and the indices of refraction (n) of substrate and the medium above the film. In this thesis, we used quartz which 1 mm thick as substrate at which n is about 1.47 at 532 nm whereas that for Fe-doped BTO is about 1.85 and for Fe-doped CCTO is about 1.95 at the same wavelength used quartz as blank substrate in the



optical transmission experiment due to its high melting temperature point and transparency, respectively.

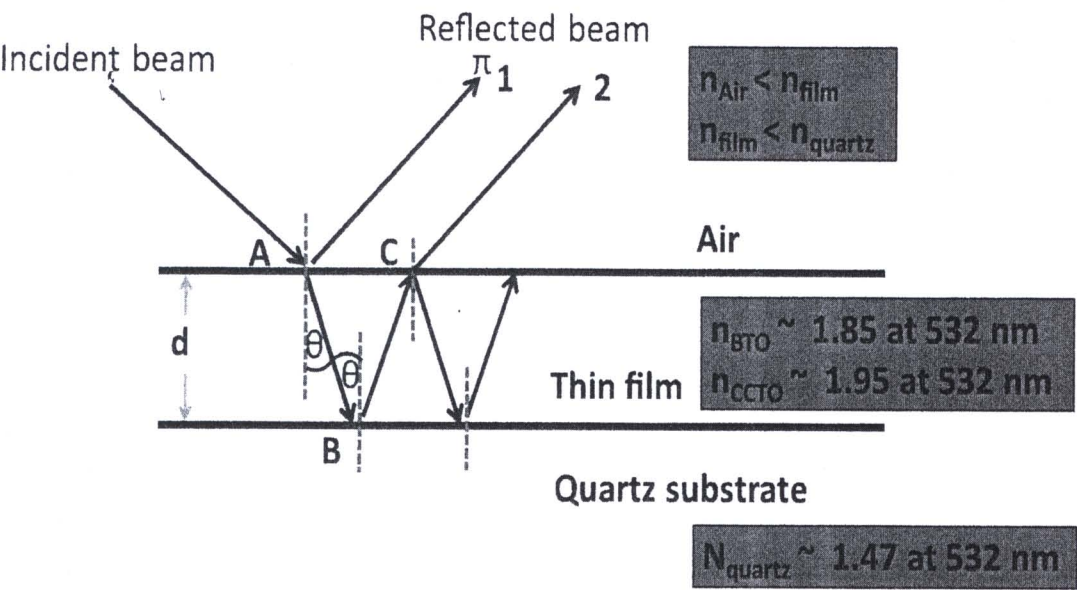


Figure 2.4: Interference between light reflecting from the film surface (1) and from the film-substrate (2) interface.

A wave traveling from a medium of refractive index n_1 toward a medium of refractive index n_2 undergoes a 180° phase change upon reflection when $n_2 > n_1$ and no phase change if $n_2 < n_1$. The wavelength of light λ_n in a medium whose refractive index n is

$$\lambda_n = \frac{\lambda}{n} \quad (2.8)$$

where λ is the wavelength of light in free space.

Since $n_{air} < n_{thin\,film}$, the reflected beam at the point A, which reflected from the upper film surface, has phase change 180° or π . The beam 2, which is reflected from the lower surface film at the point B and then transmitted through the film at the point C, have no phase change because of $n_{thin\,film} > n_{quartz}$ at the point C. Therefore, the beam 1 has the phase change of 180° relative to the beam 2. The path difference between beam 1 and beam 2 is equal to $2d\sin\theta$. When θ is small angle or the light perpendicular with the film surface, we get the condition for destructive interference

$$2n_{film}d = m\lambda \quad (2.9)$$

where $m = 0, 1, 2, \dots$

The condition for constructive interference is

$$2n_{film}d = (m + \frac{1}{2})\lambda \quad (2.10)$$

where $m = 0, 1, 2, \dots$

In Fig. 2.5, at long wavelengths (photon energies less than the band gap), the transmission (T) shows oscillations from interference effects in the transparent film. At short wavelength (photon energies greater than the band gap), the transmitted light intensity decreases to zero.

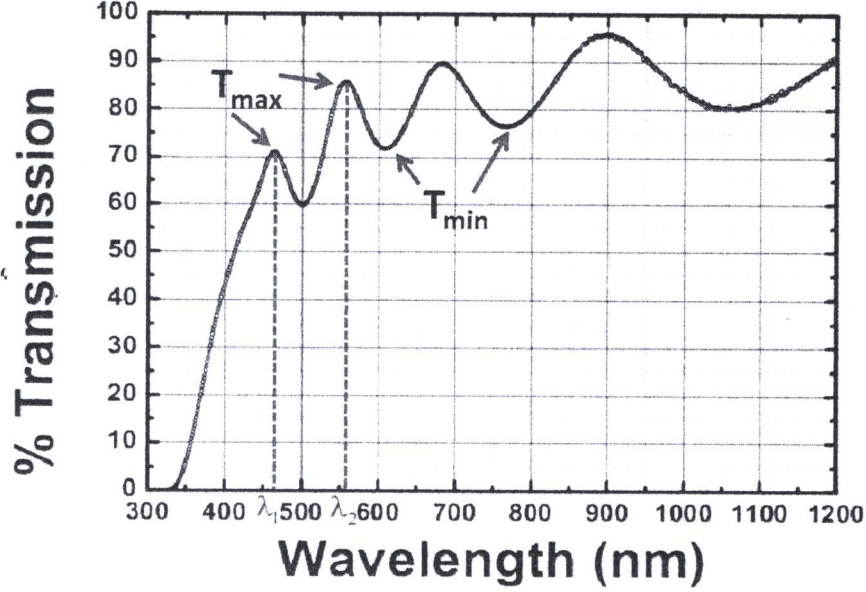


Figure 2.5: The transmission spectra of Fe-doped BTO films with 8 layers.

The notation of T_{max} and T_{min} refer to the value of the maximum and minimum in T. From equation 2.9, when we consider two maxima of the transmission patterns according to wavelengths λ_1 and λ_2 , we can write

$$2n_{film}d = (m + \frac{1}{2})\lambda_1 \quad (2.11)$$

$$2n_{film}d = (m + \frac{1}{2})\lambda_2 \quad (2.12)$$

From equation 2.11 and 2.12, we can solve for the film thickness (d) as follows:

$$d = \frac{\lambda_1 \lambda_2}{2[n(\lambda_1)\lambda_2 - n(\lambda_2)\lambda_1]} \quad (2.13)$$

2.6 Dielectric properties

In this section, we are interested in fundamentals of linear dielectric properties of matter. The relation between the dielectric constant and the dipole moment stating with the displacement field \vec{D} is shown in equation 2.14

$$\vec{D} = \varepsilon_0 \vec{E} + \vec{P} \quad (2.14)$$

where \vec{E} is macroscopic electric field, ε_0 is the vacuum permittivity and \vec{P} is the macroscopic polarization. The polarization \vec{P} and the electric field \vec{E} are related to

$$\vec{P} = \varepsilon_0 \chi \vec{E}$$

where χ is the susceptibility. Substituting for \vec{P} in equation 2.14

$$\vec{D} = \varepsilon_0(1 + \chi) \vec{E}$$

This allows to define the material's permittivity, χ , and dielectric constant, ε' :

$$\varepsilon = \varepsilon_0(1 + \chi) \rightarrow \varepsilon' = \frac{\varepsilon}{\varepsilon_0} = (1 + \chi) \quad (2.15)$$

writing $\vec{D} = \varepsilon_0 \varepsilon' \vec{E}$ and substituting in equation 2.14, we get

$$\varepsilon' - 1 = \frac{P}{\varepsilon_0 E} = \frac{M}{\varepsilon_0 V E} \quad (2.16)$$

where the polarization has been replaced with the total dipole moment of the sample (M) divided by the volume (V).